DISCOVERY
Melba M. Crawford manuscript

HIGH RESOLUTION WETLAND MAPPING VIA AIRSAR AND OPTICAL SENSORS

Melba M. Crawford[1], James C. Gibeaut[2], Shailesh Kumar[1],
Amy Neuenschwander[1], Rasih Ustun[1], K. Clint Slatton[1]
[1]Center for Space Research, The University of Texas at Austin
3925 W. Braker Lane, Suite 200, Austin, TX 78759
Ph: (512)471-7993, fax: (512)471-3570, email: crawford@csr.utexas.edu
[2]Bureau of Economic Geology, The University of Texas at Austin

Abstract

Coastal areas are often plagued by persistently cloudy conditions, so land cove
sensed data from optical sensors is extremely difficult. While land cover mapping fr
been investigated extensively in recent years, classification results using standard
those obtained from optical data. A new algorithm that handles non-Gaussian distribu
appropriate bands for each class is investigated for analyzing fully polarimetric AIR
NASA/JPL over a coastal wetland. The relative merits of AIRSAR and an optical sensor
terms of classification accuracy using the new approach. Results obtained using the
those of maximum likelihood classification and demonstrate the viability of mapping w
frequency, multi-polarization AIRSAR data.

Introduction

Classification of land cover using remotely sensed data has traditionally been
multispectral sensors that acquire data in the visible and infrared regions of the el
areas are often plagued by persistent cloud cover, thereby making it impossible to sc
these sensors reliably. The development of airborne and space-based synthetic apertu
provided a totally new capability for mapping in an all-weather, day-night environmen
from classification of SAR data using traditional methods are typically inferior to t
can be attributed to the speckle noise characteristic of SAR data, the lack of multi-
data, and the fact that the information contained in SAR data is inherently different
multispectral and hyperspectral sensors measure primarily chemistry-based responses,
be used to infer structural properties of the surface and vegetation (size, shape, an
parameters (moisture content and salinity). This study focused on mapping wetland ma
optical data acquired by CASI (Compact Airborne Spectrographic Imager) and SAR data a
NASA/JPL AIRSAR system using a new algorithm that selects the most useful bands of a
each land cover class. Joint utilization of the sensor information in a multi-sensor
investigation.

Test Site

Bolivar Peninsula, part of the low relief barrier islands of the Texas coast, i
Galveston Bay. The land cover and geomorphology of the area are being studied intens
from the Center for Space Research and the Bureau of Economic Geology of the Universi The early
stage of development of this peninsula is represented today by a series of accretiona
Two large washover fan deposits created by storm events are also present. Extensive s
inland side of Bolivar Peninsula as well as on the large fan deposits. A test site,
southern Bolivar Peninsula, is depicted in Figure 1.

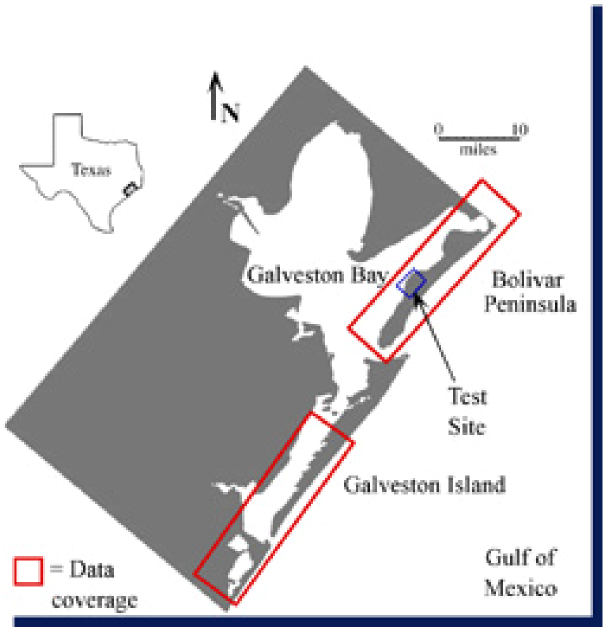

Figure 1 - Study site on Bolivar Peninsula near Galveston, Texas

The distribution of the terrain types and vegetation communities on barrier com
Peninsula is highly dependent upon their elevation relative to sea level, even though
adjacent communities is slight. Vertical relief on the peninsula occurs mostly in th
side of the peninsula. There, accretion is largely a function of sedimentary process
storms. The frequency of inundation, soil salinity, and vegetation all depend on the
dunes, which are no more than five meters higher than the swales between them, are ty
large-grained sand. The swales are often just several centimeters above the water ta
saturated with brackish water due to the salt spray from the surf. Even smaller elev
with the environments in the marshes.

At the highest elevations of the peninsula, upland vegetation consisting of tre
dominates (Figure 2), below which a hyper-saline transition zone exists near the mean
environment is characterized by extremely flat, saturated, highly saline soil with li
distal (Figure 4) and proximal (Figure 5) marshes that contain tall marsh grasses occ
At the lowest levels are the inundated mud flats with discontinuous patches of marsh
elevations of these environments differ by less than one meter in some places.

Figure 2 - Uplands shrub and herbaceous vegetation

Figure 3 - Hypersaline area with adjacent succulent vegetation

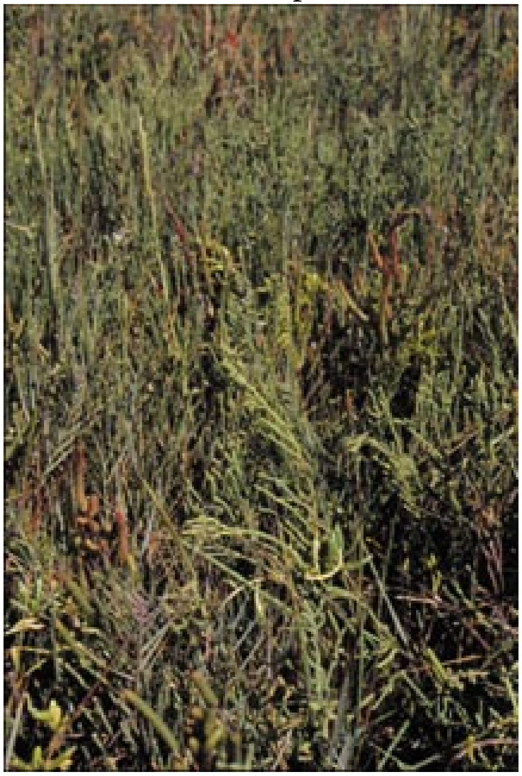

Figure 4 - High distal marsh vegetation mixtures

Figure 5 - Students acquiring spectrometer readings of high proximal marsh

Figure 6 - Low proximal marsh and mud flats

Remotely Sensed Data

Remotely sensed data were acquired over Bolivar Peninsula using a suite of inst
multispectral and hyperspectral sensors, synthetic aperture radar, and a scanning las
of hyperspectral data (448 to 804 nm) were acquired in April 1999 by CASI on a Cessna
spatial resolution of approximately four meters. Figure 7 contains a color composite
that show the delineation of the various vegetation zones.

The eleven classes identified in the CASI data include all the major land cover
classes are not always visually identifiable, and mixtures of vegetation signatures o
classes. The low proximal marsh (purple signature in these bands) immediately adjace
Waterway in the upper right corner of Figure 7 is comprised of pure stands of smooth
inundated. During the acquisition of CASI data, the inundation of this area ranged f
The signature darkens as the low proximal marsh transitions into the high proximal ma
of seashore saltgrass and marsh hay cordgrass. It was muddy, but not inundated, duri
distal marsh (reddish tan) adjacent to the high proximal marsh contains seashore salt
cordgrass. It is shown most clearly near the hyper-saline sand flats (white) that pr
side of the image. The flats are either barren or sparsely vegetated by glasswort.
vegetation including Gulf cordgrass borders the woody upland scrub (pink). Two agric
as classes: bare soil (grayish-white) and recently turned fields of hay (light green)
elms are shown in dark green along the fence lines, on the spoil island beyond the In
scattered clumps at the higher elevations of the peninsula. The parallel structures
image are vegetated dunes and associated swales. Differences between vegetation grow
swales are clearly indicated.

The NASA Jet Propulsion Laboratory (JPL) AIRSAR system acquired C (5.2 cm), L (
band data over the study area in 1995, 1996, and 1998. Figure 8 shows a three freque
(C-HH, L-HH, and L-VV) of five-meter resolution (9-look) AIRSAR data acquired at 40 M
Although the SAR sensor measures different properties than the CASI and the data exhi
noise of SAR, the image indicates the same general delineation of classes. Complex bande
the classes are exhibited as the upland shrubs on the left side of the image transiti
right. The lower marshes are actually shown more clearly in the SAR than the CASI, a
individual water bodies. The AIRSAR and CASI data were acquired in the same season,

under somewhat different tidal conditions. The water signature in CASI also appears
lowest marsh areas relative to the response in AIRSAR. Bare sand flats reflect almos
SAR antenna and thus have the same response as the radar shadow near tall grasses in

Figure 7 - CASI data
(RGB 661nm, 570nm, 491nm)

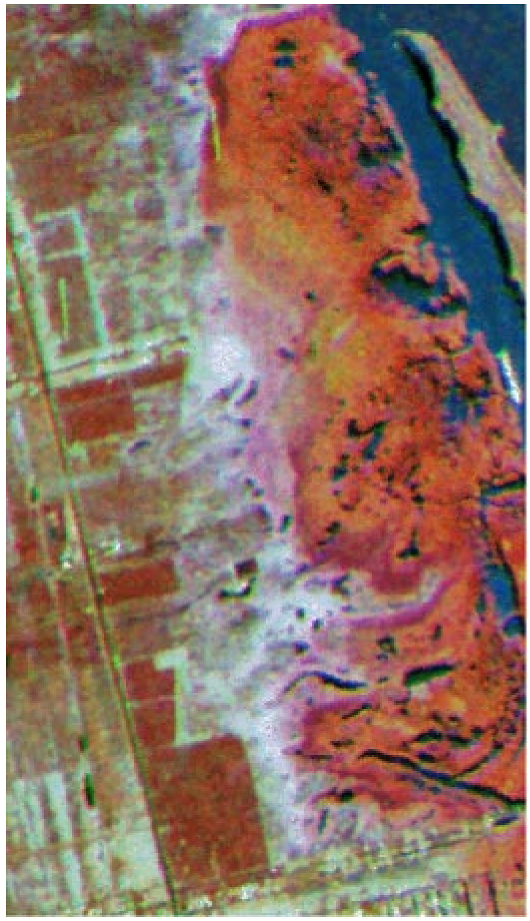

Figure 8 - AIRSAR data
(RGB: C-HH, L-HH, L-VV)

Classification Results

The CASI and AIRSAR data were first analyzed independently via maximum likeliho
observations from each class are assumed to have a multivariate Gaussian distribution
and redundancy in spectrally adjacent bands of CASI motivated the use of transformati
Components or Minimum Noise Fraction (MNF) or selection of a subset of the available
classes are often best discriminated by different band combinations, selection of a s
is problematic. Linear and circular polarizations and the phase difference between t
and L bands were investigated for classification of the AIRSAR data. The initial cl
radar data were far inferior to those obtained for optical data. Alternative approac
models (Crawford and Ricard, 1998) and hierarchical, multi-resolution approaches (Ric
investigated to mitigate the effect of speckle. Radial basis function models and mul
networks were developed to allow modeling of non-Gaussian distributed data (Crawford
classification accuracy improved using these approaches, computational requirements f
sized images were excessive when the number of bands from either AIRSAR or CASI was l

A new approach that utilizes a class dependent band selection phase for optimal
of candidate classes coupled with a Bayesian classifier based on a mixture of Gaussia
CSR group (Crawford et. al, 1999; Kumar et. al, 1999). First, parameters of a mixtur
estimated to represent the probability density function of each member in every pairw
selected for discriminating between pairs of classes based on their incremental contr
that is defined as the log-odds ratio of posterior probabilities of the two classes.
classifiers are then combined for the final classification using either a voting meth
probability rule applied to an estimate of posterior probabilities obtained from the
classifiers. The new algorithm was applied individually to the AIRSAR and CASI data.
listed in Table 1 were obtained using a threshold in the incremental gain of the rele
terminating the feature selection phase and the voting method for combining outputs o
Similar accuracies were achieved for both sensors for threshold values less than .25.

Table 1. Test Set Classification Accuracy for Single-Source Classifiers

	Class											
Sensor	1	2	3	4	5	6	7	8	9	10	11	Overal
AIRSAR	100.0	83.87	99.7	99.6	74.2	78.1	100.	99.8	67.2	98.9	100.	89.45
CASI	100.0	100.0	100.	100.	100.	100.	100.	96.5	100.	96.4	100.	99.77

Class Key: Class 1: Water; Class 2: Low Proximal Marsh; Class 3: High Proximal Marsh; Cl
Marsh; Class 5: Sand Flats; Class 6: Agriculture 1 - pasture; Class 7: Trees; Class 8
Agriculture 2 – Bare soil; Class 10: Transition; Class 11: Halophytes

Often two Gaussians were required in the class dependent multivariate distribut
CASI, thereby justifying the use of mixture distributions to appropriately represent
For both AIRSAR and CASI, the number of bands selected for discriminating between pai
one to six. Figures 9 and 10 contain the classification maps for AIRSAR and CASI res
differences in characteristics measured by the sensors were indicated in some locatio
roads to be the same class as sand flats, while in the microwave data, the response o
transition zone) in general, results were quite similar. Differences are typically r
similar “other class.” Most significantly, AIRSAR data indicated much more extensive
CASI. This is consistent with the original imagery in Figures 7 and 8.

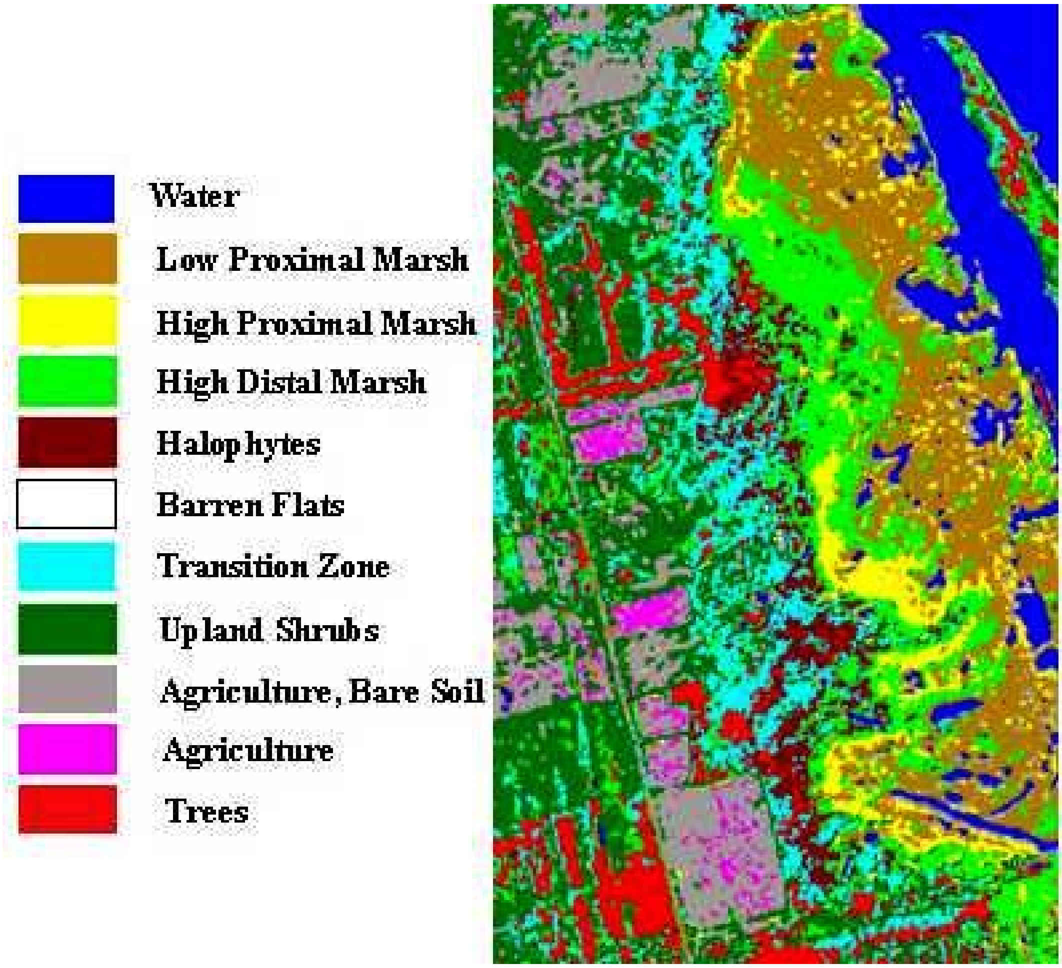

Figure 9 - Classification output of AIRSAR

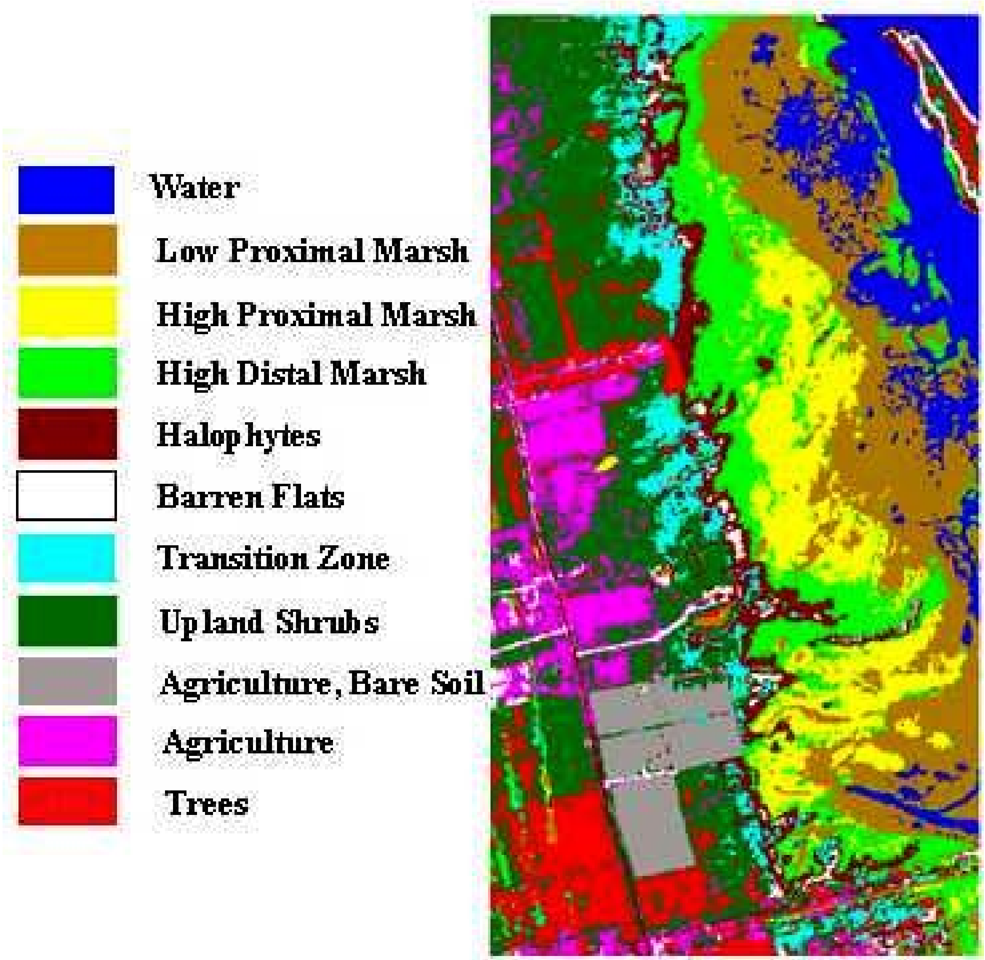

Figure 10 - Classification output of CASI

As expected, classes that are the most similar to both sensors (e.g. lower and soil and halophytes, pasture and uplands) required more bands for discrimination. Ho often differed in their respective capability to discriminate between specific classe consideration of multi-sensor mapping. For example, the scattering mechanisms for C short halophytic vegetation and the upper distal marsh vegetation are similar, while observed in CASI allow better discrimination. Similarly, sand flats were easily disc difficult to discriminate from bare soil using AIRSAR. Additionally, reliable traini extremely difficult to obtain for the AIRSAR scene. The resultant small sample size estimating parameters in the probability density function and degraded classification difficult to discriminate using either sensor, the value of the relevance function wa the number of bands that contributed significantly to the incremental relative gain i function. It should also be noted that some clearing of land occurred after the AIRS indicated in the lower left portion of the classified images. Likewise, regrowth of corner of the CASI image for fields cleared in 1998. The lower classification accura indicative of their respective within-class signature variabilities, which were confi AIRSAR data.

Classification accuracies over test data, as well as qualitative evaluation of indicate that indeed multi-frequency, multi-polarization SAR is a viable sensor for m regions. This is extremely important for all tropical and subtropical areas plagued rainfall. Indeed, for the Texas acquisitions, the initial CASI mission had to be ter the November 1998, but SAR data were actually acquired in 1996 during a rainstorm! I mapping, the longer wavelengths of SAR data proved to be extremely useful in detectin as faults, tidal creeks, and inlets as well as the presence of tidal inundation. TOP also provided topographic information that was shown to further improve some classifi 1998; Crawford et. al, 1999).

Several methods for multi-sensor classification of CASI and AIRSAR were investi analyzing a vector of combined inputs, b) combining results obtained from individual the current algorithm (Crawford et. al, 1999), and c) selecting the best sensor for a combining results for the C-class discrimination problem. Accuracy increased and the for each pairwise classifier decreased, thereby demonstrating that statistically uniq cover mapping is provided by both sensors. Research in data fusion is ongoing.

Future Research

The new classification procedure is being enhanced to include a Markov random f effects of speckle. It is also being implemented within a hierarchical scheme that w classification. In addition to classification, the AIRSAR data on Bolivar Peninsula incident angle dependent scattering model of marsh vegetation (Slatton et. al, 1996, incorporated into the classification process. Additionally, a scattering mechanism-b 1989) is being investigated in conjunction with a hierarchical classification scheme Finally, new approaches to classification that more effectively exploit the structura AIRSAR and the chemistry-based responses in optical data are being developed.

References

Crawford, M.M and M.R. Ricard, [1998], “Hierarchical Classification of SAR Data Using Model, Southwest Symp. on Image Processing, Tucson, AZ, April 1998, 81-86.

Crawford, M.M., S. Kumar, M.R. Ricard, J.C. Gibeaut, and A.L. Neuenschwander [1999], Polarimetric and Interfermetric SAR Data for Classification of Coastal Environmen Geosci. Remote Sens., GRS 37, 1306-1315.

Kumar, S., M.M. Crawford, and J. Ghosh [1999], "A Versatile Framework for Labeling Number of Classes," Proc. Int. Joint Conf. on Neural Networks, Washington, D.C., July 10-16 (public progress via CD).

Ricard, M.R. A.L. Neuenschwander, M.M. Crawford, and J.C. Gibeaut [1997], “Multisenso Wetland Environments using Airborne Multispectral and SAR Data,” Proc. 1997 Int. Geosci. and Remote Sens. Symp., Singapore, August 10-14, 667-669.

Ricard, M. and M.M. Crawford [1998], “Multiscale Hierarchical Classification of Wetla SAR Data”, Proc. 1998 Int. Geosci. and Remote Sens. Symp., Seattle, WA, , July 6-

Slatton, K.C., M.M. Crawford, J.C. Gibeaut, and R. Gutierrez [1996], “Modeling Wetlan Polarimetric SAR,” Proc. 1996 Int. Geosci. and Remote Sens. Symp., Lincoln, NE, May 27

Slatton, K.C., M.M. Crawford, J.C. Gibeaut, and R. Gutierrez, R. [1999], “Modeling SA to Coastal Inundation,” Proc. 1999 Int. Geosci. and Remote Sens. Symp., Hamburg, Germany, 2446-2448.

van Zyl, J.J. [1989], “Unsupervised Classification of Scattering Behavior Using Radar IEEE Trans. Geosci. Remote Sens., GRS-27, 36-45.